


Neuropathological features of SARS-CoV-2 delta and omicron variants

Erica Normandin, PhD,¹ Navid Valizadeh, MBBCh,² Emily A. Rudmann, BS,²
Rockib Uddin, BS,³ Sabrina T. Dobbins, MSc,¹ Bronwyn L. MacInnis, PhD,¹
Robert F. Padera, Jr, MD, PhD,⁴ Katherine J. Siddle, PhD,¹ Jacob E. Lemieux, MD, DPhil,³
Pardis C. Sabeti, MD, DPhil,¹ Shibani S. Mukerji, MD, PhD,²
Isaac H. Solomon , MD, PhD^{4*}

¹Broad Institute of MIT and Harvard, Cambridge, Massachusetts, USA

²Division of Neuroimmunology and Neuro-infectious Diseases, Department of Neurology, Massachusetts General Hospital, Boston, Massachusetts, USA

³Division of Infectious Diseases, Department of Medicine, Massachusetts General Hospital, Boston, Massachusetts, USA

⁴Department of Pathology, Brigham and Women's Hospital, Boston, Massachusetts, USA

*Send correspondence to: Isaac H. Solomon, MD, PhD, Department of Pathology, Brigham and Women's Hospital, 75 Francis Street, AL360U.2, Boston, MA 02115; E-mail: ihsolomon@bwh.harvard.edu

Shibani S. Mukerji and Isaac H. Solomon are co-senior authors and contributed equally to the study.

ABSTRACT

Severe acute respiratory syndrome coronavirus 2 (SARS-CoV-2) is continually evolving resulting in variants with increased transmissibility, more severe disease, reduced effectiveness of treatments or vaccines, or diagnostic detection failure. The SARS-CoV-2 Delta variant (B.1.617.2 and AY lineages) was the dominant circulating strain in the United States from July to mid-December 2021, followed by the Omicron variant (B.1.1.529 and BA lineages). Coronavirus disease 2019 (COVID-19) has been associated with neurological sequelae including loss of taste/smell, headache, encephalopathy, and stroke, yet little is known about the impact of viral strain on neuropathogenesis. Detailed postmortem brain evaluations were performed for 22 patients from Massachusetts, including 12 who died following infection with Delta variant and 5 with Omicron variant, compared to 5 patients who died earlier in the pandemic. Diffuse hypoxic injury, occasional microinfarcts and hemorrhage, perivascular fibrinogen, and rare lymphocytes were observed across the 3 groups. SARS-CoV-2 protein and RNA were not detected in any brain samples by immunohistochemistry, in situ hybridization, or real-time quantitative PCR. These results, although preliminary, demonstrate that, among a subset of severely ill patients, similar neuropathological features are present in Delta, Omicron, and non-Delta/non-Omicron variant patients, suggesting that SARS-CoV-2 variants are likely to affect the brain by common neuropathogenic mechanisms.

KEYWORDS: COVID-19, Delta, Neuropathology, Omicron, SARS-CoV-2

INTRODUCTION

Severe acute respiratory syndrome coronavirus 2 (SARS-CoV-2) is continually evolving and can generate variants that may lead to enhanced transmission, immune escape, or increased pathogenicity. The Delta variant (B.1.617.2 and AY lineages) of SARS-CoV-2, the dominant strain in the United States from July to mid-December of 2021, was more contagious and caused more severe disease in unvaccinated individuals than prior circulating strains (1–3). The Omicron variant (B.1.1.529 and BA lineages) has been the dominant global strain since December 2021 and has been reported to have increased transmissibility, reduced neutralization by some monoclonal antibody treatments, and reduced effectiveness of vaccination (4–6). Omicron has also been associated with

milder overall disease compared to Delta and earlier lineages, with a subset of reported hospitalizations interpreted as incidental findings (7,8).

While neurological symptoms are common in the acute and post-acute periods of SARS-CoV-2 infections, the specific effects of Delta and Omicron variants on the central nervous system are largely unknown (9–11). Prior to the emergence of the Delta variant, published autopsy reports encompassing approximately 900 patients suggested an overall picture of hypoxic-ischemic injury, hemorrhage, microvascular disruption, and nonspecific inflammation (12–16). Hypoxic ischemic injury and acute to subacute microinfarcts to large territorial infarcts have been reported in a subset of cases in the majority of published studies (17–31), as have a variety of hemorrhagic

lesions involving brain parenchyma and overlying meninges (17,19–24,26,30,32–36). These lesions are likely nonspecific, which is supported by a recent study that did not identify differences in staining for amyloid precursor protein, a marker suggestive of agonal hypoxia-ischemia, between Coronavirus disease 2019 (COVID-19) cases and controls (19). Typical histological findings of viral encephalitis including microglial nodules, neuronophagia, and lymphocytic inflammation are largely absent, while predominance of microglial cells, particularly in the brainstem, is favored to be a nonspecific finding in septic or otherwise critically ill patients (17,19–26,28,29,31,32,36–39). Rare reports of demyelination reminiscent of acute disseminated encephalomyelitis and acute hemorrhagic leukoencephalitis have been described, which may represent postinfectious manifestations of SARS-CoV-2 infection (17,20,21,30,40,41).

Most studies using commercially available nucleocapsid and spike antibodies did not identify positive cellular staining for SARS-CoV-2 in brain tissue with the exception of rare cells reported as positive in the brainstem or cranial nerves. Minimal if any viral RNA has been detected from brain tissue by quantitative real-time PCR or digital droplet PCR (18,20,23–33,38,42). Given concerns for increased severity of disease and decreased treatment and vaccination effectiveness with the Delta and Omicron variants compared to earlier circulating variants, we report the neuropathological findings from 12 Delta variant and 5 Omicron variant autopsies and compare them to 5 non-Delta/non-Omicron variant COVID-19 patients, including examination of SARS-CoV-2 protein and RNA using immunohistochemistry (IHC), in situ hybridization (ISH), and quantitative reverse transcriptase-polymerase chain reaction (RT-qPCR).

MATERIALS AND METHODS

Patient cohort

Ethical approval was obtained from the Mass General Brigham institutional review board with waived informed consent for the use of excess tissue not needed for diagnostic purposes (IRB 2015P001388). Patients with positive nasopharyngeal swab SARS-CoV-2 RT-PCR testing with postmortem brain examination at Brigham and Women's Hospital from April 1, 2020 to February 15, 2022 were screened for inclusion in this study. Suspected SARS-CoV-2 Delta variant cases were identified by first reported COVID-19 symptoms or positive RT-PCR test between July 1 and December 15, 2021. Suspected Omicron variant cases with first reported symptoms from December 16, 2021 to February 15, 2022 were also identified. Following viral genome sequencing (see below), 2 cases in the Omicron variant-predominant time period were identified as Delta variant and reassigned to the Delta variant cohort. Presumed non-Delta/non-Omicron-variant autopsy cases performed between April 1 and December 31, 2020 were reviewed and roughly matched for age and approximate duration of illness. Detailed neuropathological findings for 3 non-Delta/non-Omicron variant patients (Patients 1–3) were previously reported (31). Demographics, laboratory, imaging, and clinical data were extracted from the electronic medical record.

Data analysis and construction of Figure 1 were performed in R (version 4.1.1) (43) and using BioRender.

Autopsy procedure and gross examination

Autopsies were performed in a negative pressure isolation room by personnel equipped with powered air-purifying or N95 respirators. Bone saws fitted with vacuum filters were used to open skulls to minimize potential for aerosolization of viral particles. Brains were then removed, weighed fresh, and partially or wholly fixed in 10% formalin for 3–8 days prior to gross examination.

Histopathological evaluation

A standard set of brain tissue sections were submitted for microscopic evaluation in all cases, including (1) inferior frontal lobe with olfactory tract/bulb(s), (2) cingulate gyrus with corpus callosum, (3) hippocampus at level of lateral geniculate nucleus, (4) occipital lobe with primary visual cortex, (5) anterior basal ganglia, (6) thalamus, (7) cerebellum, (8) midbrain, (9) pons, and (10) medulla. Tissue sections were processed and paraffin embedded using standard protocols. Hematoxylin and eosin stains were examined for all blocks. Hypoxic injury was defined by the presence of neurons with eosinophilic cytoplasm and pyknotic nuclei or of ghost neurons, and graded as mild (rare cells), moderate (scattered clusters of cells), or severe (frequent or diffuse involvement, e.g. pseudolaminar necrosis). IHC for SARS-CoV-2 nucleocapsid protein (NB100-56576; Novus Biologicals, Centennial, CO; 1:500 dilution), SARS-CoV-2 spike protein (GTX632604; GeneTex, Irving, CA; 1:1000 dilution), CD45/LCA (M0701; Dako, Glostrup, Denmark; 1:600 dilution), CD68 (PG-M1; Dako; 1:200 dilution), CD61 (2f2 Cell Marque, Rocklin, CA; 1:250 dilution), and fibrinogen (ab58207; Abcam, Cambridge, UK; 1:2000 dilution) was performed on formalin-fixed paraffin-embedded (FFPE) tissue sections of frontal lobe/olfactory nerve, thalamus, and medulla for all cases. SARS-CoV-2 spike RNA ISH (RNAscope 2.5 LS Probe V-nCoV2019-S; Advanced Cell Diagnostics, Newark, CA) was performed on the same sections as viral IHC using the Leica Bond system according to manufacture protocols.

Nucleic acid extraction and RT-qPCR SARS-CoV-2 quantification

For each FFPE sample, total nucleic acids were extracted from 3 20- μ m scrolls using a QuickDNA/RNA FFPE Miniprep kit (Zymo R1009, Irvine, CA) according to manufacturer's instructions. Water and pre-COVID-19-era autopsy brain tissue samples were used as negative controls for the extraction. RNA was isolated by enzymatic digestion of DNA (Thermo Fisher AM2238, Waltham, MA) followed by nucleic acid purification (Beckman Coulter, Brea, CA), then eluted in 15 μ L water. SARS-CoV-2 nucleocapsid protein-targeting RT-qPCR (based on the US CDC N1 assay) was performed for each sample and controls. The CDC assay cycling conditions were altered for compatibility with SYBR assays (48°C for 30 minutes for reverse transcription and 98°C for 10 minutes for activation, followed by 45 cycles of PCR at 95°C for 10 seconds, 60°C for 45 seconds). In triplicate, 1 μ L of viral

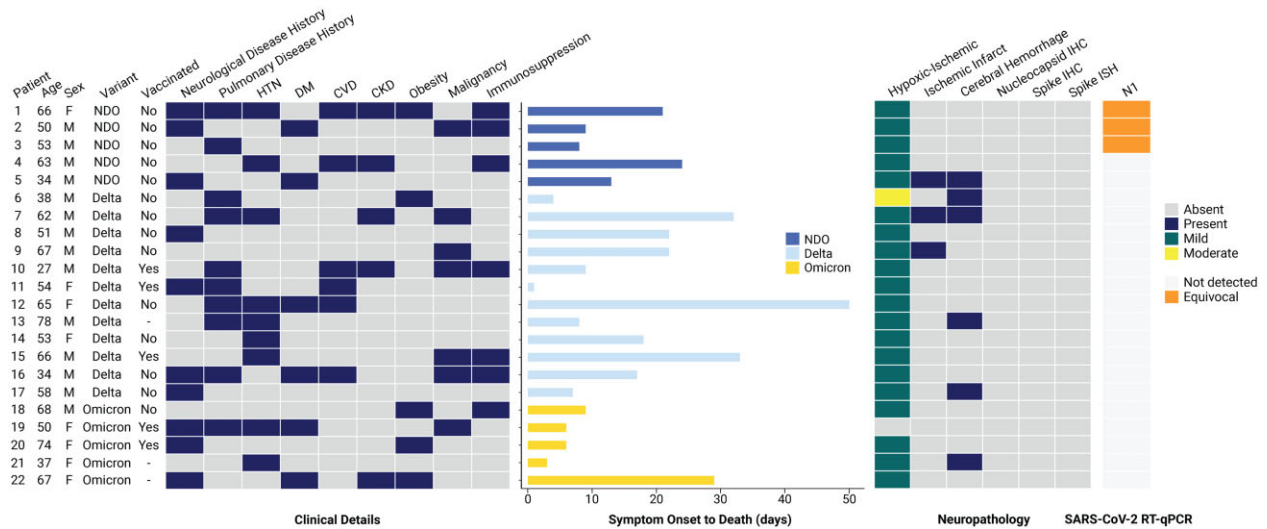


Figure 1. Clinical characteristics and neuropathologic features of SARS-CoV-2 Delta, Omicron, and non-Delta/non-Omicron variants. Heat maps from left to right show clinical details including patient age, sex, SARS-CoV-2 variant, vaccination status, comorbidities, and duration of illness, neuropathologic features including hypoxia-ischemic changes, ischemic infarct, and cerebral hemorrhage, virus nucleocapsid and spike immunohistochemistry, spike RNA in situ hybridization, and RT-qPCR using probes for the nucleocapsid (N1) gene target. CKD, chronic kidney disease; CVD, cardiovascular disease; DM, diabetes mellitus; HTN, hypertension; IHC, immunohistochemistry; ISH, in situ hybridization; NDO, non-Delta/non-Omicron; RT-qPCR, real-time quantitative polymerase chain reaction; N1, nucleocapsid gene (based on the US CDC N1 probes).

RNA (diluted 1:3) was added to a 10 μ L reaction, which included TaqPath (Thermo Fisher) with 500 nM of each primer and 125 nM of probe. SARS-CoV-2 synthetic DNA was used as a standard curve, and water and pre-COVID-19-era autopsy brain tissue samples were used as negative controls for the RT-qPCR assay. For each reaction, if the fluorescent signal crossed threshold, then the cycle at which that occurred was reported (Ct). The concentration of viral RNA was calculated from the mean of available Ct measurements using the standard curve, and then corrected for the dilution factor. Viral loads were quantified only for samples with all 3 replicates yielding a Ct, and considered other samples equivocal (1 or 2 replicates yielding a Ct) or negative (zero replicates yielding a Ct).

Amplicon sequencing, SARS-CoV-2 genome assembly, and lineage determination

SARS-CoV-2 variants were determined by tiled amplicon sequencing of autopsy lung FFPE tissue using the ARTIC v4 primer set. Briefly, following extraction, cDNA was synthesized from 2.5 μ L of purified RNA using random primers (Thermo Fisher). Sequencing libraries were prepared using the COVID-Seq assay kit (Illumina, San Diego, CA) with dual unique indexes (Illumina). Libraries were then purified (Beckman Coulter), quantified (Agilent Technologies, Santa Clara, CA), and pooled in equimolar amounts, then sequenced on a MiSeq v2 (Illumina) 2 \times 150 base pairs. Sequencing reads were demultiplexed using the publicly available viral-ngs demux_-only pipeline (dockstore.org/organizations/BroadInstitute/collections/pgs), as implemented on Terra platform (app.terra.bio). SARS-CoV-2 genome assembly was performed using the viral-ngs assemble_refbased pipeline, using the SARS-CoV-2 reference NC_045512.2. We observed minimal SARS-

CoV-2 sequence (<15% unambiguous genomes assembled) from negative controls (including pre-COVID-19-era autopsy tissue from lung, and water controls added at the extraction and sequencing stages), likely representing minor contamination introduced during sequencing. SARS-CoV-2 lineage determination, performed on genomes with >20% unambiguous SARS-CoV-2 base pairs, was performed using Nextclade (v2.8.1) web interface, against the full database of genomes available as of November 15, 2022. Sequences are deposited in GeneBank BioProject: PRJNA720544 (Accessions SAMN31929242-SAMN31929253).

Whole-genome sequencing was also performed on nasopharyngeal swabs at the time of infection from a subset of cases, collected at Brigham and Women's Hospital. Libraries were prepared and purified using the COVIDSeq Test Kit (Illumina), quantified using a Qubit 4 Fluorometer (Thermo Fisher) and 4150 TapeStation System (Agilent), and then sequenced using a NextSeq 2000 (Illumina) 2 \times 150 base pairs. Genomes were demultiplexed and assembled using the publicly available viral-ngs sarscov2_illumina_full pipeline (dockstore.org/organizations/BroadInstitute/collections/pgs) on Terra platform (app.terra.bio). Sequences with an assembly length greater than 24,000 base pairs were considered complete genomes and were then assigned pango lineages using the most up-to-date version of the pangoLEARN assignment algorithm. Sequences are deposited in GeneBank BioProject: PRJNA759255 (Accessions: OL675845.1, ON186330.1, ON423072.1, ON186333.1, and ON186334.1).

RESULTS

All 22 patients included in this study were positive for SARS-CoV-2 by pre-mortem nasopharyngeal swab nucleic acid

amplification tests, with the exception of Patient 11, who was positive by postmortem screening performed prior to autopsy. Five non-Delta/non-Omicron variant COVID-19 autopsy cases were performed between April 12, 2020 and December 31, 2020 (Patients 1–5). Twelve total Delta variant autopsies were performed, including 10 cases between July 12, 2021 and December 2, 2022 (Patients 6–15), and 2 additional cases during the Omicron variant-predominant time period (January and February 2022) (Patients 16–17). Five Omicron variant autopsies were performed between December 30, 2021 and February 4, 2022 (Patients 18–22). Evidence of COVID-19 pneumonia, including acute to organizing diffuse alveolar damage was observed for all cases, with the exceptions of Patient 11 (Delta variant) and Patient 19 (Omicron variant), and RT-qPCR was positive from autopsy lung tissue for all cases except Patient 11 (Supplementary Data Table S1). Amplicon sequencing of autopsy lung tissue confirmed non-Delta/non-Omicron lineages A.2 (Patient 1), B.1 (Patients 2 and 3), and B.1.2 (Patients 4 and 5). Delta lineages were confirmed for 7/12 Delta variant cases including AY.86 (Patient 6), AY.119 (Patients 7 and 15), AY.47 (Patient 8), AY.117 (Patient 10), B.1.617.2 (Patient 16), and AY.25 (Patient 17). The remaining presumed

Delta variant patients and all presumed Omicron variant patients yielded insufficient SARS-CoV-2 RNA sequencing reads for genotyping. Sequencing of pre-mortem nasopharyngeal swabs was performed for 5 patients, confirming 1 additional Delta variant patient with AY.3 (Patient 12) and 4 Omicron variant patients with BA.1.1 (Patients 18 and 21), BA.1.15 (Patient 19), and BA.1 (Patient 20) (Supplementary Data Table S1).

Clinical characteristics, laboratory data, and autopsy findings for Delta, Omicron, and non-Delta/non-Omicron variant patient groups are summarized in Table 1. Small numbers of patients in the groups precluded detection of statically significant differences; however, some general trends were noted. Median age at death was slightly higher for Omicron variant patients at 67 (interquartile range [IQR] 50–68) years compared to Delta variant (56 [IQR 48–65] years) and non-Delta/non-Omicron variant (53 [IQR 50–63] years) patients (Tables 1 and 2). Duration of illness, determined by first reported symptoms was slightly shorter for Omicron variant patients (median [IQR] 6 [6–9] days) compared to Delta (18 [IQR 8–25] days) and non-Delta/non-Omicron (13 [IQR 9–21] days) variant patients. The Omicron variant group comprised of more women (n = 4, 80%), and were exclusively

Table 1. Summary of clinical characteristics, laboratory data, and autopsy findings^a

	Non-Delta/Non-Omicron (n = 5)	Delta (n = 12)	Omicron (n = 5)
Genotype confirmed by sequencing, No. (%)	5 (100)	8 (67)	4 (80)
Clinical characteristics			
Age at death, median [IQR], years	53 [50–63]	56 [48–65]	67 [50–68]
Sex, No. (% male)	4 (80)	9 (75)	1 (20)
Race/Ethnicity, No. (% White, non-Hispanic)	4 (80)	6 (67)	0 (0)
Vaccination, No. (%)	0 (0)	3 (25)	2 (40)
Illness duration, median [IQR], days	13 [9–21]	18 [8–25]	6 [6–9]
Laboratory data			
Max CRP, median [IQR], mg/L	198 [114–284]	111 [56–175]	120 [117–163]
Max ferritin, median [IQR], µg/L	4618 [1124–9373]	3064 [2977–10 521]	293 [217–8583]
Max D-dimer, median [IQR], ng/mL	4000 [3068–4000]	4000 [2341–4000]	3213 [2479–3607]
AST, median [IQR], U/L	69 [68–140]	116 [65–485]	28 [24–191]
ALT, median [IQR], U/L	109 [27–138]	58 [44–276]	19 [13–34]
GFR, median [IQR], mL/min/1.73 m ²	16 [14–21]	28 [26–59]	29 [29–61]
WBC, median [IQR], K/µL	16.4 [3.2–19.4]	15.7 [10.1–26.6]	11.3 [6.2–12.2]
ANC, median [IQR], K/µL	4.0 [2.1–7.5]	13.9 [8.2–18.9]	8.8 [4.9–9.5]
ALC, median [IQR], K/µL	0.24 [0.17–0.51]	1.00 [0.59–3.70]	0.75 [0.39–2.15]
INR, median [IQR]	1.5 [1.4–2.1]	1.3 [1.1–2.7]	1.7 [1.4–2.0]
Autopsy findings			
Postmortem interval, median [IQR], h	40 [20–52]	44 [28–62]	72 [69–96]
Brain weight, median [IQR], g	1460 [1380–1530]	1325 [1243–1400]	1180 [1150–1280]
Hypoxic-ischemic injury, n (%)	5 (100)	12 (100)	4 (80)
Infarction, n (%)	1 (20)	2 (17)	0 (0)
Hemorrhage, n (%)	1 (20)	4 (33)	1 (20)
Microglial nodules, n (%)	0 (0)	2 (17)	0 (0)
Thrombi, n (%)	0 (0)	0 (0)	0 (0)
Nucleocapsid IHC, n (%)	0 (0)	0 (0)	0 (0)
Spike IHC, n (%)	0 (0)	0 (0)	0 (0)
Spike RNA ISH, n (%)	0 (0)	0 (0)	0 (0)
N1 RT-qPCR, n (%)	0 (0)	0 (0)	0 (0)

^a Laboratory results reflect last measured values prior to death unless otherwise specified.

Normal ranges: CRP 0.0–10.0 mg/L; ferritin female: 13–150 and male 30–400 µg/L; D-dimer <500 ng/mL; AST 10–50 (U/L), ALT 10–50 (U/L); GFP >59 ml/min/1.73 m²; WBC 4.00–10.00 K/µL; ANC 2.50–6.00 K/µL; ALC 1.00–4.80 K/µL; INR 0.9–1.1.

ALC, absolute lymphocyte count; ANC, absolute neutrophil count; ALT, alanine aminotransferase; AST, aspartate aminotransferase; CRP, C-reactive protein; GFR, glomerular filtration rate; INR, international normalized ratio; WBC, white blood cell count.

Table 2. Demographics, clinical history, neurological symptoms, and treatment

Pt. no.	Age	Sex	Race/Ethnicity	Medical history	Neuro.symptoms	Neuro-imaging	SARS-CoV-2 vaccination status	COVID-19 treatments	MV
1	66	F	Black, not Hispanic	Obesity, CAD, HF, CKD, RA-SLE, ILD, MGUS, bipolar, PVD, HTN	None	None	Unvaccinated	Tocilizumab, hydroxychloroquine	PPV
2	50	M	White, not Hispanic	ALL, bone marrow transplant, DM, neuropathy, depression	Headache	None	Unvaccinated	Dexamethasone, tocilizumab	PPV
3	53	M	White, not Hispanic	OSA, EtoH use disorder	Weakness, myalgias	None	Unvaccinated	Hydrocortisone, tocilizumab	PPV
4	63	M	White, not Hispanic	CAD, HTN, HLD, CKD, cardiac transplant	None	None	Unvaccinated	Dexamethasone, remdesivir, casirivimab/imdevimab	PPV
5	34	M	White, not Hispanic	DM, depression, EtOH cirrhosis	Seizure, encephalopathy (hepatic encephalopathy)	Head CT normal	Unvaccinated	Dexamethasone	PPV
6	38	M	Asian	Obesity, asthma	Anoxic brain injury	Head CT diffuse edema	Unvaccinated	Methylprednisolone	PPV
7	62	M	White, not Hispanic	HTN, HLD, OSA, BCC, nephrectomy, EtOH use disorder	Headache	None	Unvaccinated	Dexamethasone, remdesivir, tocilizumab	ECMO; PPV
8	51	M	NA	Remote TBI, gout, chronic pain, arthritis, tibia fracture	Syncope	None	Unvaccinated	Dexamethasone, remdesivir, tocilizumab	PPV
9	67	M	White, not Hispanic	HLD, prostate Ca	Seizure vs syncope	None	Unvaccinated	Dexamethasone, remdesivir	PPV
10	27	M	White, not Hispanic	Congenital heart disease, COPD, lymphoma, ESKD, renal transplant, CVID	None	None	Moderna (×3; 10 days prior to admission)	Dexamethasone, remdesivir, tocilizumab	PPV
11	54	F	White, not Hispanic	HCM, HLD, asthma, fibromyalgia, GERD, IBD	None	None	Pfizer ×2	None	None
12	65	F	White, Hispanic	DM, HTN, HFpEF, asthma, cirrhosis, thrombocytopenia	None	None	Unvaccinated	Dexamethasone	None
13	78	M	White, not Hispanic	HTN, COPD, BPD, cirrhosis	Disorder of consciousness	Head CT subdural hematoma	NA	None	None
14	53	F	NA	HTN, overactive bladder	None	None	Unvaccinated	Dexamethasone, remdesivir, tocilizumab	PPV

(continued)

Table 2. (continued)

Pt. no.	Age	Sex	Race/Ethnicity	Medical history	Neuro.symptoms	Neuro-imaging	SARS-CoV-2 vaccination status	COVID-19 treatments	MV
15	66	M	Black, not Hispanic	HTN, mantle cell lymphoma on rituxumab, HBV	None	None	Pfizer ×3	Dexamethasone, remdesivir, casirivimab/imdevimab	PPV
16	34	M	Asian	Huntington's disease	None	None	Unvaccinated	Dexamethasone, remdesivir	None
17	58	M	NA	HTN, HLD, GERD	Coma	None	Unvaccinated	None	PPV
18	68	M	Other, Hispanic	DM, HFrEF, PE, cervical spondylosis, relapsed ALL with SCT, SCT, skin/liver/gut GVHD, nephrolithiasis, GERD	Stupor	Head CT nonspecific white matter hypodensities	Unvaccinated	Hydrocortisone, remdesivir, casirivimab/imdevimab	PPV
19	50	F	Black, Hispanic	Obesity, pulmonary HTN, asthma, sickle cell anemia	None	None	Pfizer ×2	Dexamethasone, remdesivir	None
20	74	F	Other, Hispanic	DM, HTN, HLD, PE, depression, metastatic cholangiocarcinoma, GERD	Encephalopathy	None	Moderna ×2	Dexamethasone	None
21	37	F	Black, not Hispanic	Obesity, asthma, idiopathic intracranial hypertension, migraine, depression	None	None	NA	None	None
22	67	F	NA	DM, obesity, hypothyroidism, dementia, EtOH use disorder, CKD	Encephalopathy	NA	NA	NA	NA

ALL, acute lymphoblastic leukemia; BCC, basal cell carcinoma; CKD, chronic kidney disease; COPD, chronic obstructive lung disease; CVID, common variable immunodeficiency; DM, diabetes mellitus; ECMO, extracorporeal membrane oxygenation; EtOH use disorder, alcohol use disorder; HF, heart failure; HLD, hyperlipidemia; HTN, hypertension; ILD, interstitial lung disease; MGUS, monoclonal gammopathy of undetermined significance; MV, mechanical ventilation; NA, not available; OSA, obstructive sleep apnea; PPV, positive pressure ventilation; PVD, peripheral vascular disease; RA-SLE, rheumatoid arthritis-systemic lupus erythematosus; TBI, traumatic brain injury.

Black (n = 2, 40%) and/or Hispanic (n = 3, 60%), compared to Delta variant or non-Delta/non-Omicron variant patients who were majority White, non-Hispanic and male. All patients had at least 1 significant comorbidity (Fig. 1; Table 2), with a slightly higher number of conditions in non-Delta/non-Omicron variant patients (4 [IQR 2–4]) than Delta (2.5 [IQR 1–4]) or Omicron (2 [IQR 2–4]) variant patients. The most common comorbidities for non-Delta/non-Omicron variant patients were history of immunosuppression (3/5, 60%) and prior neurological disease (3/5, 60%), followed by preexisting pulmonary disease (2/5, 40%), hypertension (2/5, 40%), diabetes mellitus (2/5, 40%), cardiovascular disease (2/5, 40%), and chronic kidney disease (2/5, 40%). Delta variant patients most commonly had preexisting pulmonary disease (7/12, 58%), followed by hypertension (5/12, 42%), malignancy (5/12, 42%), cardiovascular disease (4/12, 33%), and prior neurological disease (4/12, 33%). Omicron variant patients most commonly had prior neurological illness (3/5, 60%) and obesity (3/5, 60%), followed by hypertension (2/5, 40%) and diabetes mellitus (2/5, 40%).

Neurological symptoms were observed in 6/12 (50%) Delta variant patients including headache, syncope, seizure versus syncope, disorder of consciousness, coma, and anoxic brain injury, 3/5 (60%) Omicron variant patients including stupor and encephalopathy, and 3/5 (60%) non-Delta/non-Omicron variant patients including headache, weakness, myalgia, seizure, and encephalopathy (Table 2). Neuroimaging was limited to head computed tomography in 4 patients, showing diffuse edema (Patient 6) and subdural hematoma (Patient 13) in 2 Delta variant patients, nonspecific white matter hypodensities in 1 Omicron variant patient (Patient 18), and no significant findings in 1 non-Delta/non-Omicron variant patient (Patient 5) (Table 2).

Three of 12 (25%) Delta variant and 2/5 (40%) Omicron variant patients received 2 or 3 doses of Moderna or Pfizer mRNA vaccines (Tables 1 and 2). Eight (67%) of the Delta patients had mechanical ventilation, 9 (75%) received steroids, 7 (58%), remdesivir, 4 (33%) tocilizumab, and 1 (8%) casirivimab/imdevimab monoclonal antibodies. One (20%) Omicron variant patient had mechanical ventilation, 3 (60%) received

Table 3. Neuropathological findings

Patient no.	SARS-CoV-2 pango lineage	Symptom onset to death (days)	Postmortem interval (h)	Brain weight (g)	COVID-19-associated neuropathological findings
1	A.2	21	52	1290	Mild hypoxic ischemic injury
2	B.1	9	40	1460	Mild hypoxic ischemic injury
3	B.1	8	20	1530	Mild hypoxic ischemic injury
4	B.1.2	24	10	1590	Mild hypoxic ischemic injury
5	B.1.2	13	116	1380	Scattered petechial/microhemorrhages; acute microinfarct in inferior olivary nucleus; mild hypoxic ischemic injury
6	AY.86 (Delta)	4	41	1460	Focal subarachnoid hemorrhage; mild to moderate hypoxic ischemic injury
7	AY.119 (Delta)	32	50	1580	Scattered microinfarcts with hemorrhage involving white matter throughout brain; focal microglial nodule formation in medulla; mild hypoxic ischemic injury
8	AY.47 (Delta)	22	58	1370	Mild hypoxic ischemic injury
9	Unknown (presumed Delta) ^a	22	43	1260	Chronic microinfarct in corpus callosum; mild hypoxic ischemic injury
10	AY.117 (Delta)	9	30	1210	Mild hypoxic ischemic injury
11	Unknown (presumed Delta) ^a	1	122	1290	Mild hypoxic ischemic injury
12	AY.3 (Delta)	50	8	1020	Mild hypoxic ischemic injury
13	Unknown (presumed Delta) ^a	8	180	1250	Subdural hemorrhage; mild hypoxic ischemic injury
14	Unknown (presumed Delta) ^a	18	45	1390	Single microglial nodule in medulla; mild hypoxic ischemic injury
15	AY.119 (Delta)	33	11	1220	Mild hypoxic ischemic injury
16	B.1.617.2 (Delta)	17	72	1430	Mild hypoxic ischemic injury
17	AY.25 (Delta)	7	20	1360	Mild hypoxic ischemic injury; red blood cell extravasation
18	BA.1.1 (Omicron)	9	96	1380	Mild hypoxic ischemic injury
19	BA.1.15 (Omicron)	6	69	1280	None
20	BA.1 (Omicron)	6	65	1180	Mild hypoxic ischemic injury
21	BA.1.1 (Omicron)	3	72	1100	Parenchymal microhemorrhages; subarachnoid hemorrhage; mild hypoxic ischemic injury
22	Unknown (presumed Omicron) ^a	29	121	1150	Mild hypoxic ischemic injury

^a SARS-CoV-2 variant not confirmed by sequencing of lung tissue or nasopharyngeal swabs. These cases were assigned to Delta variant cohort if first reported COVID-19 symptoms or positive RT-PCR test were between July 1 and December 15, 2021 or to Omicron cohort if first reported symptoms or positive RT-PCR test were from December 16, 2021 to February 15, 2022.

steroids, 2 (40%) remdesivir, and 1 (20%) casirivimab/imdevimab. Multiple laboratory values including max C-reactive protein, ferritin, and D-Dimer, and last recorded alanine aminotransferase, aspartate aminotransferase, international normalized ratio, white blood cell count, and absolute neutrophil count were elevated in a subset of patients across all groups, while glomerular filtration rate and absolute lymphocyte count were abnormally decreased (Table 1; Supplementary Data Table S2).

Detailed gross and microscopic neuropathological examination was performed for all cases (Fig. 1; Table 3). Small numbers of patients in the groups precluded detection of statically significant differences; however, multiple abnormalities were noted. Mild to moderate hypoxic injury was seen in all cases except Patient 19 (Omicron variant). Subdural hemorrhage was identified in 1 (8%) Delta variant patient (Patient 13), focal subarachnoid hemorrhage in 1 (8%) Delta variant patient (Patient 6), and 1 (20%) Omicron variant patient (Patient

21), and white matter microhemorrhages in 2 (17%) Delta variant patients (Patients 7 and 17), 1 (20%) Omicron variant patient (Patient 21), and 1 (8%) non-Delta/non-Omicron case (Patient 5) (Fig. 2). Microinfarcts were identified in 2 (17%) Delta variant patients (Patients 7 and 9) and 1 (20%) non-Delta/Non-Omicron variant patient (Patient 5). While occasional clusters of intravascular platelets were present, no thrombi were identified by H&E or CD61 IHC in any of the sections (Fig. 3). Qualitatively similar degrees of perivascular fibrinogen staining were observed between Delta, Omicron, and non-Delta/non-Omicron variant patients (Fig. 3). CD45 and CD68 IHC highlighted rare perivascular lymphocytes and microglia distributed diffusely throughout the brain parenchyma in all slides (Fig. 4).

IHC to detect SARS-CoV-2 nucleocapsid and spike antigens, and ISH to detect SARS-CoV-2 spike RNA were performed on multiple brain regions. Viral staining was negative in neurons, glia, endothelium, and immune cells in the frontal

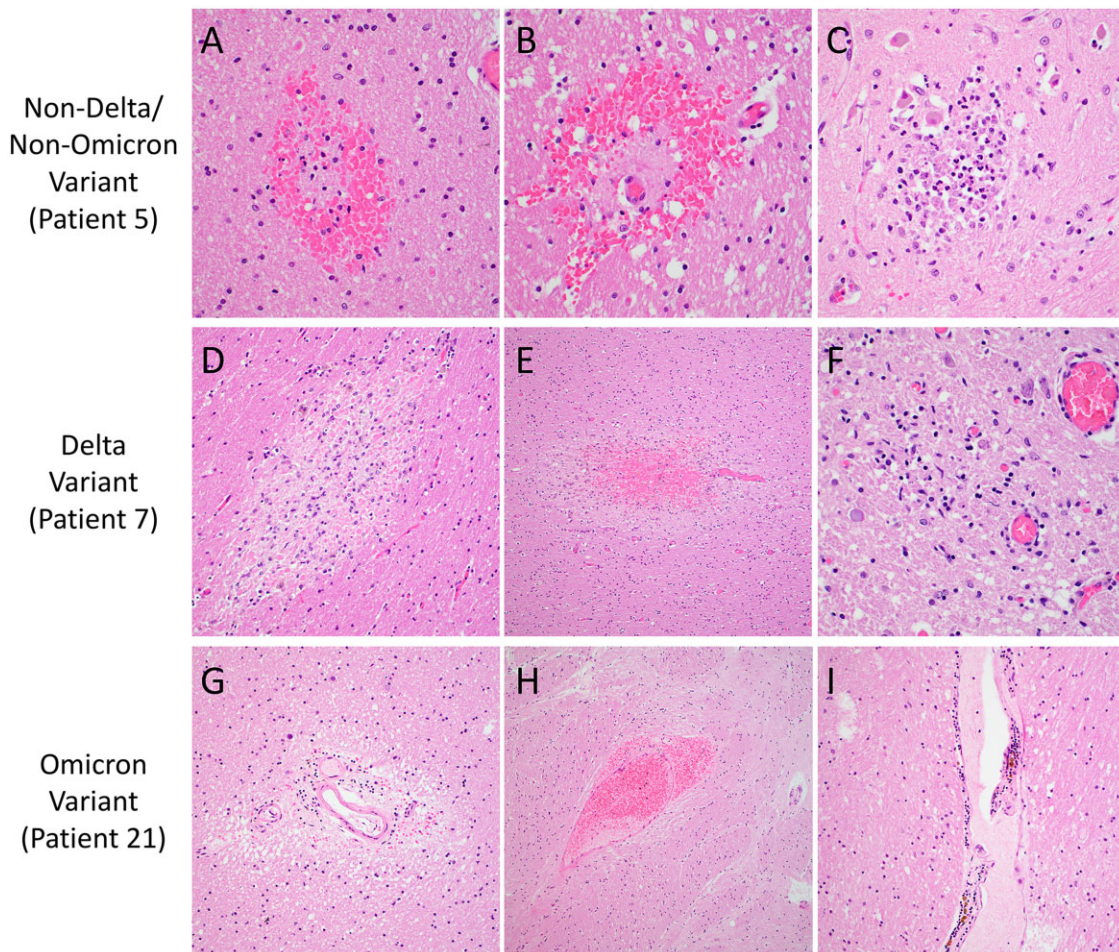


Figure 2. Neuropathologic features of SARS-CoV-2 Delta, Omicron, and non-Delta/non-Omicron variant patients. Representative images show microhemorrhages in the occipital lobe (A) and basal ganglia (B) and a microinfarct in the medulla (C) of a non-Delta/Non-Omicron variant patient (Patient 5). A microinfarct in the midbrain (D), a microhemorrhage in the temporal lobe (E), and a microglial nodule in the medulla (F) are shown for a Delta variant patient (Patient 7). Perivascular rarefaction in the corpus callosum (G), perivascular microhemorrhage/red blood cell extravasation in the basal ganglia (H), and mild perivascular inflammation in the thalamus (I) are illustrated for an Omicron variant patient (Patient 21). Images taken with 40× objective (A–C, F), 20× (D, G, I), and 10× (E, H).

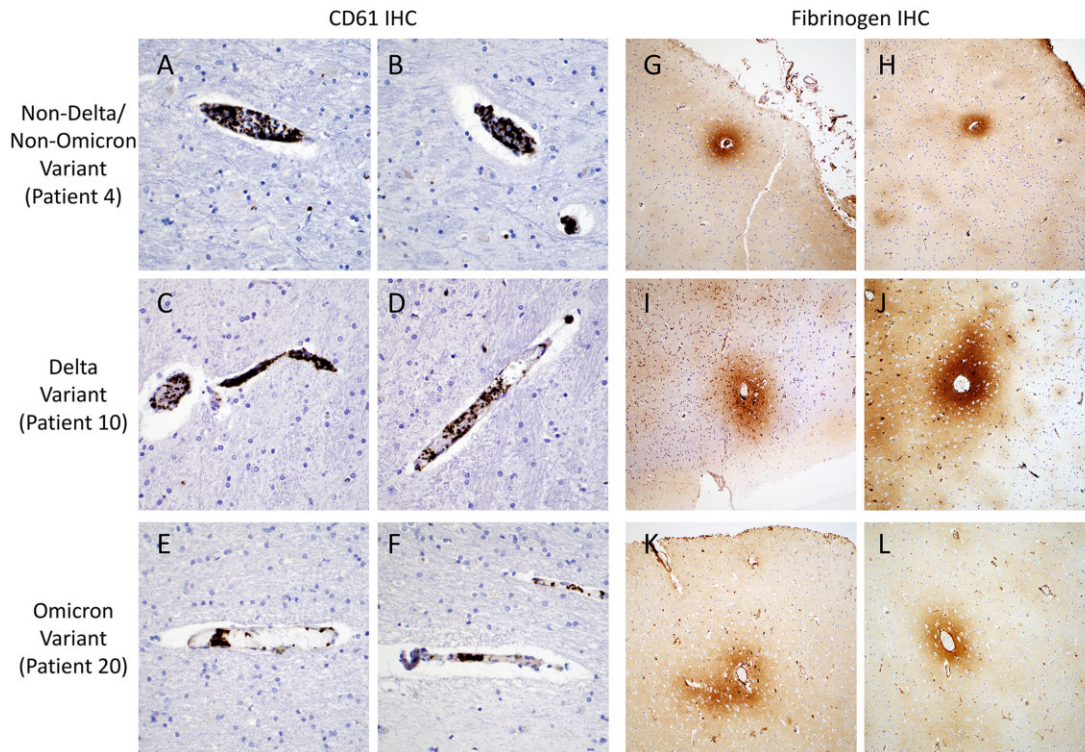


Figure 3. Intravascular platelet aggregates and perivascular fibrinogen staining. Representative CD61 immunohistochemistry images (A–F) highlight intravascular aggregates of platelets in a non-Delta/Non-Omicron variant patient (A, B, Patient 4), a Delta variant patient (C, D, Patient 10), and an Omicron variant patient (E, F, Patient 20). Representative fibrinogen immunohistochemistry images (G–L) highlight perivascular staining in a non-Delta/Non-Omicron variant patient (G, H, Patient 4), a Delta variant patient (I, J, Patient 10), and an Omicron variant patient (K, L, Patient 20). Images A–F taken with 40× objective, and images G–L taken with 10× objective.

lobe with olfactory nerve, thalamus, and medulla for all of the cases (Fig. 5; Supplementary Data Table S3). RT-qPCR for SARS-CoV-2 nucleocapsid RNA was performed on the same brain regions and was negative or below the limit of detection in all cases (Fig. 1; Supplementary Data Table S3).

DISCUSSION

Postmortem examination of brains from 12 Delta, 5 Omicron, and 5 non-Delta/non-Omicron variant patients who died within 51 days of the onset of COVID-19 symptoms, 60% with documented neurological symptoms, showed similar findings of diffuse hypoxic injury, occasional microinfarcts and hemorrhage, perivascular fibrinogen, and rare lymphocytes. These findings are in keeping with prior studies of COVID-19 neuropathology, which reported hypoxic injury, acute to subacute microinfarcts and large territorial infarcts, subdural, subarachnoid, and parenchymal hemorrhages, sparse perivascular lymphocytic inflammation, and variable numbers of microglia, present in varying combinations in a subset of cases (17–39). No evidence of virus was identified by nucleocapsid or spike IHC, spike ISH, or by N1 RT-qPCR of brain tissue despite ample evidence of infection with Delta and Omicron variants in lung tissue. Viral load was quantified from FFPE tissue, which can have decreased sensitivity compared to fresh or frozen samples due to RNA quality and fragmentation. Performance of N1 RT-qPCR (73-bp target) as a single assay could

also decrease sensitivity and specificity, although these have been shown to have high concordance with other gene targets and histopathological findings (31,44). Equivocal or low-levels of viral RNA in brain tissue has been reported for non-Delta/non-Omicron variants; their clinical relevance remains unclear given that the majority of reports are unable to identify the cellular source of virus using standard histopathological and ultrastructural techniques (12,18,20,23–33,38,42,45). In this study, neither viral RNA nor protein was identified in brain tissue of the Delta or Omicron variant patients despite evidence of microvascular injury and microglial infiltration, supporting a non-neuroinvasive mechanism of neuropathogenesis.

Few studies to date have compared the neuropathological findings amongst different SARS-CoV-2 variants, and none, to the best of our knowledge, included Delta or Omicron variants. A pair of studies in Italy and Switzerland reported increased microthrombi with acute/subacute ischemic damage, and increased microhemorrhages earlier in the pandemic (February to May 2020), with more frequent leptomeningeal chronic inflammation in later waves (October 2020 to April 2021) (26,46). Similar viral loads were detected between SARS-CoV-2 B.1.1.7 (Alpha) and prior variants in a German case series (47). Mouse and hamster models of COVID-19 show decreased severity of disease for Omicron variant, and conflicting results as to whether the effects of Delta variant are decreased compared to earlier strains of SARS-CoV-2 (48,49). Similar to these animal models, we observed a range of

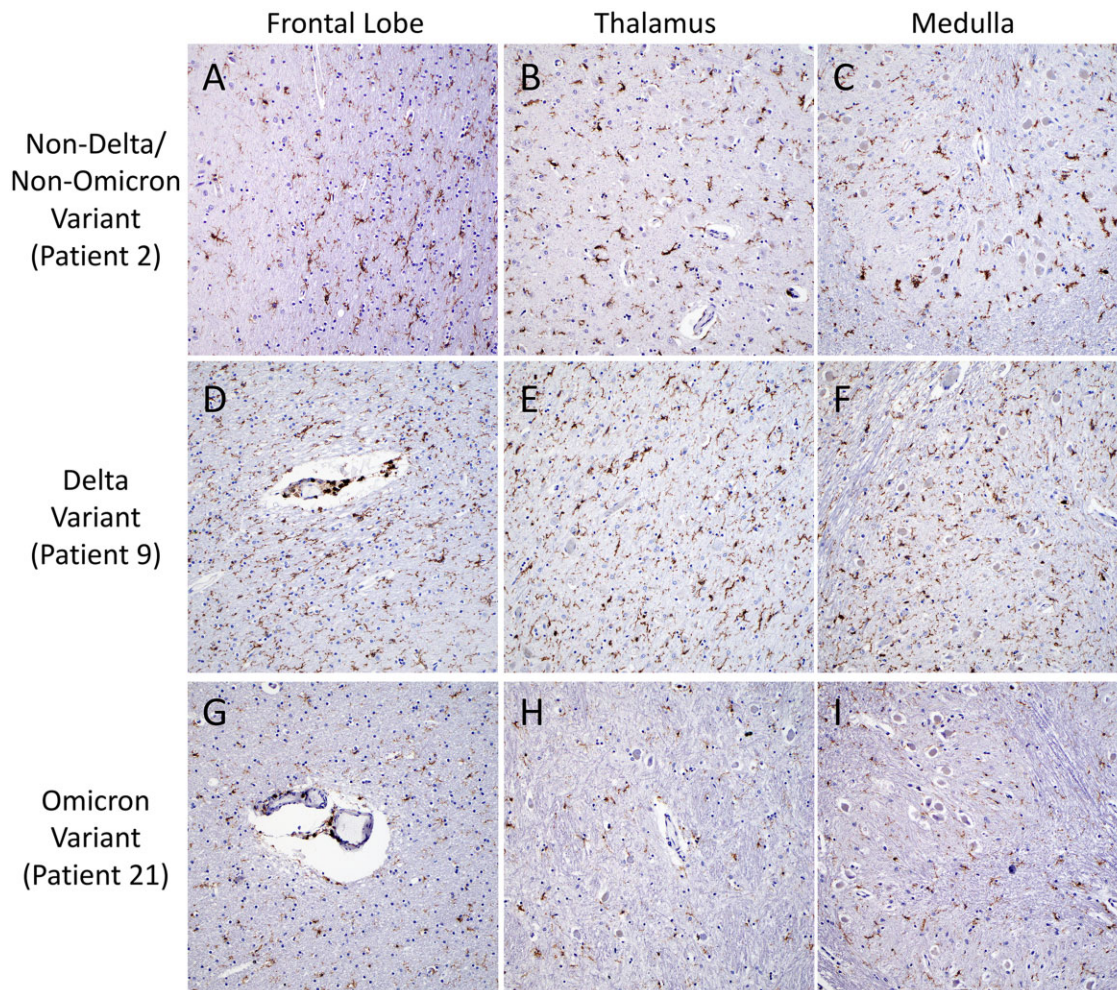


Figure 4. Microglial predominant inflammatory infiltrates. Representative images of CD45 immunohistochemistry highlight diffuse microglia and occasional perivascular lymphocytes in the frontal lobe (A, D, G), thalamus (B, E, H), and medulla (C, F, I), of a non-Delta/non-Omicron variant patient (A–C, Patient 2), a Delta variant patient (D–F, Patient 9), and an Omicron variant patient (G–I, Patient 21). All images taken with 10× objective.

findings for Delta and Omicron variant patients that overlapped with prior SARS-CoV-2 variants. Confirming genotyping using whole-genome sequencing resulted in reclassification of Omicron cases as Delta even during the Omicron period. This is not surprising given differences in virulence among SARS-CoV-2 variants and highlights the importance of obtaining the genotype of cases for accurate classification in study of disease pathology. Four out of 12 (33%) presumed Delta and 1/5 (20%) presumed Omicron cases were unable to be confirmed by genotyping, raising the possibility of misclassification; however, these specific cases were collected after the transition periods between dominant strains (>99% prevalence), minimizing this potential source of error.

A major factor confounding the interpretation of clinical and neuropathological differences between variants is the evolving treatment protocols and availability of SARS-CoV-2 vaccines. SARS-CoV-2 mRNA vaccination has been shown to be protective against severe disease both in Delta and Omicron variants (50). Only 3/12 (25%) Delta variant patients in this study were vaccinated, 2 of whom likely gained suboptimal

protection due to immunocompromised status (Patients 10 and 15), while the third exhibited no evidence of COVID-19 pneumonia or detectable virus in lung tissue by RT-qPCR (Patient 11). Two of 5 (40%) Omicron variant patients were vaccinated; one died from diffuse gastrointestinal ischemia and hemorrhage in the setting of sickle cell disease with acute vaso-occlusive crisis without evidence of COVID-19 pneumonia (Patient 19); the other died with COVID-19 pneumonia in the setting of widely metastatic cholangiocarcinoma (Patient 20). Mild hypoxic ischemic injury was the sole neuropathological finding in 4/5 (80%) of the vaccinated patients, suggesting that vaccination does provide some protection for the central nervous system against COVID-19, which may be attributable to lower viral titers or less severe pulmonary/systemic disease. The individual impact of COVID-19 treatments including corticosteroids, tocilizumab, remdesivir, and monoclonal antibodies (casirivimab/imdevimab) on neuropathological findings is less clear due to the multitude of treatment combinations and overall evolution of best clinical practices throughout the pandemic.

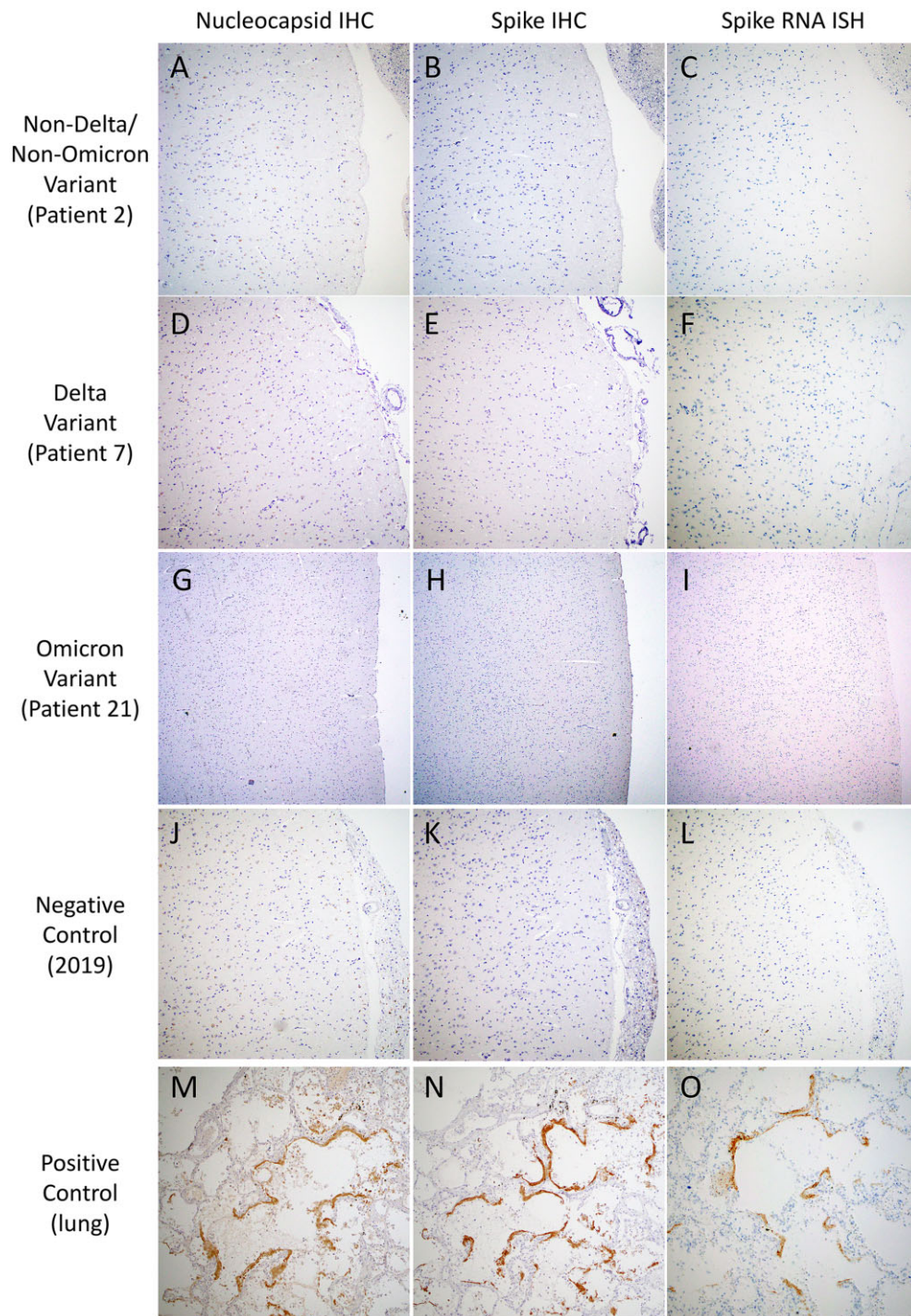


Figure 5. SARS-CoV-2 immunohistochemistry and in situ hybridization. Representative images of SARS-CoV-2 nucleocapsid immunohistochemistry (IHC) (A, D, G, J, M), SARS-Cov-2 spike IHC (B, E, H, K, N), and SARS-CoV-2 spike RNA in situ hybridization (ISH) (C, F, I, L, O) in frontal lobe sections from a non-Delta/Non-Omicron variant patient (A–C, Patient 2), a Delta variant patient (D–F, Patient 7), an Omicron variant patient (G–I, Patient 21), a 2019 pre-COVID-19-era negative control patient (J–L), and positive control autopsy lung from a non-Delta/Non-Omicron variant patient (M–O). All images taken with 10× objective.

While these findings are based on a limited number of cases from a single academic institution, with inherent variability in comorbidities, disease duration, and treatments precluding detection of statistically significant differences, they do suggest that SARS-CoV-2 variants and earlier lineages are likely to

affect the brain by similar mechanisms in severe, fatal infections. However, the specificity of the observed findings cannot be directly attributed to COVID-19 rather than general features of critically ill patients due to the lack of a COVID-19-negative control cohort in this study. The neuropathological

impact of variants requires further study in the acute setting, and remains to be determined in the post-acute setting.

FUNDING

Research reported in this study was supported in part by the National Institute of Neurological Disorders and Stroke, the National Institute of Allergy and Infectious Diseases, and the National Institute of Mental Health of the National Institutes of Health under awards R21NS119660 (IHS), U19AI110818 (PCS), and K23MH115812 (SSM), James S. McDonnell Foundation, and Rappaport Fellowship (SSM), the U.S. Food and Drug Administration contract (HHSF223201810172C; PCS), the U.S. Centers for Disease Control and Prevention (75D30120C09605; BLM), and the Howard Hughes Medical Institute (PCS).

ACKNOWLEDGMENTS

The authors would like to thank the patients and their families. They also wish to thank members of the Brigham and Women's Hospital Autopsy Service (Michelle Siciliano, John Grzyb, Jacob Plaisted, and Jane Wakefield), Neuropathology Laboratory (Karen Bryan and Sebastian Valentin), and Clinical Immunohistochemistry Laboratory (Mei Zheng, Alyson Campbell, and Geraldine Pinkus), as well as the staff of the Dana-Farber/Harvard Cancer Center Specialized Histopathology Core (supported in part by an NCI Cancer Center Support Grant # NIH 5 P30 CA06516).

CONFLICT OF INTEREST

PCS is a founder, consultant, and shareholder of Sherlock Biosciences and DelveDx, and a board member and shareholder of Danaher Corporation. PCS holds several patents relevant to infectious disease diagnostics and genome sequencing. No other disclosures are reported.

SUPPLEMENTARY DATA

[Supplementary Data](https://academic.oup.com/jnen) can be found at academic.oup.com/jnen.

REFERENCES

- Lambrou AS, Shirk P, Steele MK, et al.; Strain Surveillance and Emerging Variants NS3 Working Group. Genomic surveillance for SARS-CoV-2 variants: predominance of the delta (B.1.617.2) and omicron (B.1.1.529) variants—United States, June 2021–January 2022. *MMWR Morb Mortal Wkly Rep* 2022;71:206–11
- Taylor CA, Patel K, Pham H, et al.; COVID-NET Surveillance Team. Severity of disease among adults hospitalized with laboratory-confirmed COVID-19 before and during the period of SARS-CoV-2 B.1.617.2 (Delta) predominance—COVID-NET, 14 States, January–August 2021. *MMWR Morb Mortal Wkly Rep* 2021;70:1513–9
- Del Rio C, Malani PN, Omer SB. Confronting the delta variant of SARS-CoV-2, Summer 2021. *JAMA* 2021;326:1001–2
- Karim SSA, Karim QA. Omicron SARS-CoV-2 variant: a new chapter in the COVID-19 pandemic. *Lancet* 2021;398:2126–8
- Planas D, Saunders N, Maes P, et al. Considerable escape of SARS-CoV-2 Omicron to antibody neutralization. *Nature* 2022;602:671–5
- Taylor CA, Whitaker M, Anglin O, et al.; COVID-NET Surveillance Team. COVID-19-associated hospitalizations among adults during SARS-CoV-2 delta and omicron variant predominance, by Race/Ethnicity and Vaccination Status—COVID-NET, 14 States, July 2021–January 2022. *MMWR Morb Mortal Wkly Rep* 2022;71:466–73
- Nyberg T, Ferguson NM, Nash SG, et al.; COVID-19 Genomics UK (COG-UK) consortium. Comparative analysis of the risks of hospitalisation and death associated with SARS-CoV-2 omicron (B.1.1.529) and delta (B.1.617.2) variants in England: a cohort study. *Lancet* 2022;399:1303–12
- Bager P, Wohlfahrt J, Bhatt S, et al.; Omicron-Delta study group. Risk of hospitalisation associated with infection with SARS-CoV-2 omicron variant versus delta variant in Denmark: an observational cohort study. *Lancet Infect Dis* 2022;22:967–76
- Chou SH, Beghi E, Helbok R, et al.; GCS-NeuroCOVID Consortium and ENERGY Consortium. Global incidence of neurological manifestations among patients hospitalized with COVID-19—a report for the GCS-NeuroCOVID Consortium and the ENERGY Consortium. *JAMA Netw Open* 2021;4:e2112131
- Ross Russell AL, Hardwick M, Jeyantham A, et al. Spectrum, risk factors and outcomes of neurological and psychiatric complications of COVID-19: a UK-wide cross-sectional surveillance study. *Brain Commun* 2021;3:fcab168
- Marquez C, Kerkhoff AD, Schrom J, et al. COVID-19 symptoms and duration of rapid antigen test positivity at a community testing and surveillance site during pre-delta, delta, and omicron BA.1 periods. *JAMA Netw Open* 2022;5:e2235844
- Mukerji SS, Solomon IH. What can we learn from brain autopsies in COVID-19? *Neurosci Lett* 2021;742:135528
- Lin LC, Hollis B, Hefti MM. Neuropathology of COVID-19. *Indian J Pathol Microbiol* 2022;65:S146–52
- Jonigk D, Werlein C, Acker T, et al. Organ manifestations of COVID-19: what have we learned so far (not only) from autopsies? *Virchows Arch* 2022;481:139–59
- Cosentino G, Todisco M, Hota N, et al. Neuropathological findings from COVID-19 patients with neurological symptoms argue against a direct brain invasion of SARS-CoV-2: a critical systematic review. *Eur J Neurol* 2021;28:3856–65
- Lou JJ, Movassaghi M, Gordy D, et al. Neuropathology of COVID-19 (neuro-COVID): clinicopathological update. *Free Neuropathol* 2021;2:2
- Bryce C, Grimes Z, Pujadas E, et al. Pathophysiology of SARS-CoV-2: the Mount Sinai COVID-19 autopsy experience. *Mod Pathol* 2021;34:1456–67
- El Jamal SM, Pujadas E, Ramos I, et al. Tissue-based SARS-CoV-2 detection in fatal COVID-19 infections: sustained direct viral-induced damage is not necessary to drive disease progression. *Hum Pathol* 2021;114:110–19
- Serrano GE, Walker JE, Tremblay C, et al. SARS-CoV-2 brain regional detection, histopathology, gene expression, and immunomodulatory changes in decedents with COVID-19. *J Neuropathol Exp Neurol* 2022;81:666–95
- Thakur KT, Miller EH, Glendinning MD, et al. COVID-19 neuropathology at Columbia University Irving Medical Center/New York Presbyterian Hospital. *Brain* 2021;144:2696–708
- Wierzbica-Bobrowicz T, Krajewski P, Tarka S, et al. Neuropathological analysis of the brains of fifty-two patients with COVID-19. *Folia Neuropathol* 2021;59:219–31
- Colombo D, Falasca L, Marchioni L, et al. Neuropathology and inflammatory cell characterization in 10 autopsied COVID-19 brains. *Cells* 2021;10:2262
- Lopez G, Tonello C, Osipova G, et al. Olfactory bulb SARS-CoV-2 infection is not paralleled by the presence of virus in other central

- nervous system areas. *Neuropathol Appl Neurobiol* 2022;48:e12752
24. Poloni TE, Medici V, Moretti M, et al. COVID-19-related neuropathology and microglial activation in elderly with and without dementia. *Brain Pathol* 2021;31:e12997
 25. Gagliardi S, Poloni ET, Pandini C, et al. Detection of SARS-CoV-2 genome and whole transcriptome sequencing in frontal cortex of COVID-19 patients. *Brain Behav Immun* 2021;97:13–21
 26. Fabbri VP, Riefolo M, Lazzarotto T, et al. COVID-19 and the brain: the neuropathological Italian experience on 33 adult autopsies. *Biomolecules* 2022;12:629
 27. Meinhardt J, Radke J, Dittmayer C, et al. Olfactory transmucosal SARS-CoV-2 invasion as a port of central nervous system entry in individuals with COVID-19. *Nat Neurosci* 2021;24:168–75
 28. Ruz-Caracuel I, Pian-Arias H, Corral I, et al. Neuropathological findings in fatal COVID-19 and their associated neurological clinical manifestations. *Pathology* 2022;54:738–45
 29. Matschke J, Lutgehetmann M, Hagemann C, et al. Neuropathology of patients with COVID-19 in Germany: a post-mortem case series. *Lancet Neurol* 2020;19:919–29
 30. Eschbacher KL, Larsen RA, Moyer AM, et al. Neuropathological findings in COVID-19: an autopsy cohort. *J Neuropathol Exp Neurol* 2022;82:21–8
 31. Solomon IH, Normandin E, Bhattacharyya S, et al. Neuropathological features of Covid-19. *N Engl J Med* 2020;383:989–92
 32. Lee MH, Perl DP, Nair G, et al. Microvascular injury in the brains of patients with Covid-19. *N Engl J Med* 2021;384:481–3
 33. Hirschbuhl K, Dintner S, Beer M, et al. Viral mapping in COVID-19 deceased in the Augsburg autopsy series of the first wave: a multiorgan and multimethodological approach. *PLoS One* 2021;16:e0254872
 34. Mikhaleva LM, Cherniaev AL, Samsonova MV, et al. Pathological features in 100 deceased patients with COVID-19 in correlation with clinical and laboratory data. *Pathol Oncol Res* 2021;27:1609900
 35. Bugra A, Das T, Arslan MN, et al. Postmortem pathological changes in extrapulmonary organs in SARS-CoV-2 RT-PCR-positive cases: a single-center experience. *Ir J Med Sci* 2022;191:81–91
 36. Santana MF, Frank CHM, Almeida TVR, et al. Hemorrhagic and thrombotic manifestations in the central nervous system in COVID-19: a large observational study in the Brazilian Amazon with a complete autopsy series. *PLoS One* 2021;16:e0255950
 37. Jackson NR, Zeigler K, Torrez M, et al. New Mexico's COVID-19 experience. *Am J Forensic Med Pathol* 2021;42:1–8
 38. Lee MH, Perl DP, Steiner J, et al. Neurovascular injury with complement activation and inflammation in COVID-19. *Brain* 2022;145:2555–68
 39. Deigendesch N, Sironi L, Kutza M, et al. Correlates of critical illness-related encephalopathy predominate postmortem COVID-19 neuropathology. *Acta Neuropathol* 2020;140:583–6
 40. Walker JM, Gilbert AR, Bieniek KF, et al. COVID-19 patients with CNS complications and neuropathologic features of acute disseminated encephalomyelitis and acute hemorrhagic leukoencephalopathy. *J Neuropathol Exp Neurol* 2021;80:628–31
 41. Manzano GS, McEntire CRS, Martinez-Lage M, et al. Acute disseminated encephalomyelitis and acute hemorrhagic leukoencephalitis following COVID-19: systematic review and meta-synthesis. *Neurol Neuroimmunol Neuroinflamm* 2021;8:e1080
 42. Stein SR, Ramelli SC, Grazioli A, et al. SARS-CoV-2 infection and persistence in the human body and brain at autopsy. *Nature* 2022;612:758–63
 43. R Core Team. *R: A Language and Environment for Statistical Computing*. Vienna, Austria: R Foundation for Statistical Computing; 2022. <https://www.r-project.org/>.
 44. Lu X, Wang L, Sakthivel SK, et al. US CDC real-time reverse transcription PCR panel for detection of severe acute respiratory syndrome coronavirus 2. *Emerg Infect Dis* 2020;26:1654–65
 45. Dittmayer C, Laue M. Continued false-positive detection of SARS-CoV-2 by electron microscopy. *Ann Neurol* 2022;92:340–1
 46. Maccio U, Zinkernagel AS, Schuepbach R, et al. Long-term persisting SARS-CoV-2 RNA and pathological findings: lessons learnt from a series of 35 COVID-19 autopsies. *Front Med (Lausanne)* 2022;9:778489
 47. Ondruschka B, Heinrich F, Lindenmeyer M, et al. Multiorgan tropism of SARS-CoV-2 lineage B.1.1.7. *Int J Legal Med* 2021;135:2347–9
 48. Seehusen F, Clark JJ, Sharma P, et al. Neuroinvasion and neurotropism by SARS-CoV-2 variants in the K18-hACE2 mouse. *Viruses* 2022;14:1020
 49. Bauer L, Rissmann M, Benavides FFW, et al. In vitro and in vivo differences in neurovirulence between D614G, delta and omicron BA.1 SARS-CoV-2 variants. *Acta Neuropathol Commun* 2022;10:124
 50. Stowe J, Andrews N, Kirsebom F, et al. Effectiveness of COVID-19 vaccines against omicron and delta hospitalisation, a test negative case-control study. *Nat Commun* 2022;13:5736